Synthesis and Characterization of the Oxynitride $Y_2Mo_2O_{4.5}N_{2.5}$ Pyrochlore: A Neutron Diffraction and Magnetic Study

M. J. Martínez-Lope, M. T. Casais, and J. A. Alonso

Instituto de Ciencia de Materiales de Madrid, CSIC, Cantoblanco, 28049 Madrid, Spain

Reprint requests to Prof. Dr. J. A. Alonso. E-mail: ja.alonso@icmm.csic.es

Z. Naturforsch. **61b,** 164 – 169 (2006); received October 14, 2005

A new molybdenum oxynitride $Y_2Mo_2O_{4.5}N_{2.5}$ with cubic pyrochlore structure ($a = 10.3350(2)$ Å, space group $Fd\bar{3}m$, $Z = 8$) has been synthesized by heating the parent $Y_2Mo_2O_7$ oxide in flowing ammonia at 898 K. The polycrystalline sample has been characterized by thermal analysis, X-ray and neutron diffraction (NPD), and magnetic susceptibility measurements. The analysis of high resolution NPD data, based on the contrast existing between the scattering lengths of O and N, shows that both atoms are distributed at random at the anion substructure; the refined crystallographic formula implies an oxidation state of +5.25 for Mo cations. The thermogravimetric curve shows a weight gain of 7.5% at 1000 K in air, corresponding to the complete elimination of N_2 and oxidation to Mo(VI) oxide, in good agreement with the proposed composition. The magnetic susceptibility exhibits a Pauli-like, temperature-independent term which derives from the partial delocalization of Mo electrons on Mo-(O,N) bands with a broader bandwidth, as a consequence of the significant opening of the Mo-(O,N)-Mo angle and strengthening of the Mo-(O,N) interactions with respect to the parent $Y_2Mo_2O_7$ oxide. As in this oxide, a reminiscent spin-glass behaviour is observed at low temperature.

Key words: Oxynitride, Pyrochlore Structure, Neutron Diffraction, Ammonolysis, Pauli Susceptibility

Introduction

The pyrochlore structure, of general stoichiometry $A_2B_2O_6O'$, is recognized to have a great flexibility concerning the large variety of cations that can be accommodated at both A and B cationic substructures [1]. Most of the transition metals can be located at the B octahedral positions, whereas rare-earth or semimetal *p*-elements are usually comfortable at the larger A positions. This flexibility accounts for the variety in electrical and magnetic properties, going from the insulating and paramagnetic behaviour (for instance, in $RE_2Ti_2O_7$, RE: rare earths) to the metallic or half-metallic character and ferromagnetic behaviour, as observed in $Tl_2Mn_2O_7$, with colossal magnetoresistance properties [2, 3].

An alternative approach to modify or tune the physical properties of pyrochlores is by introducing different anions at the oxygen substructure. The mineral "pyrochlore" itself, (Na,Ca)(Nb,Ta)O_6F/OH, contains O^{2-}, F^- and OH^- at the anion substructure [1]. In $Cd_2Nb_2O_7$, Pannetier *et al.* [4] reported that some of the oxygen atoms can be replaced by S^{2-}, producing a phase that exhibits ferroelectricity at high temperature [5]. The introduction of N^{3-} anions has been explored much less. There have been reports of the formation of tantalum oxynitride [6, 7] and titanium oxynitride pyrochlores [8]; recently the first molybdenum oxynitride pyrochlore $Sm_2Mo_2O_{3.83}N_{3.17}$ was synthesized by Veith *et al.* [9], obtained by ammonolysis of the precursor pyrochlore oxide $Sm_2Mo_2O_7$ in flowing ammonia. The sample is semiconducting and the temperature-dependent magnetic susceptibility follows a Curie-Weiss behaviour.

Ammonolysis of transition-metal oxides has been widely used to produce oxynitrides in chemical processes in which ammonia behaves as a nitriding agent and additionally induces a change in the oxidation state of the involved transition metals. In general, this replacement at the anion substructure induces an increase in the covalency of the crystal structure, and brings about an electron delocalization effect, although yielding more insulating materials as a consequence of the strong perturbation of the periodic potential at the anion substructure [9]. From the structural point of view, oxynitrides often show the same structural type as the parent oxides for moderate substitutional rates. However, the higher charge of the nitride N^{3-}

0932–0776 / 06 / 0200–0164 $ 06.00

ion leads in general to lower cation-to-anion ratios in complex nitrides with respect to complex oxides [10]. This fact, coupled with the lower oxidising power of nitrogen as compared to oxygen, leads to the difficulty of forming completely nitrided perovskites (ABN_3) or pyrochlores ($A_2B_2N_7$): oxynitrides with partial nitrogen content are preferentially obtained [11].

An important question arises about the precise location of the nitrogen atoms and their role in the structural arrangement of oxynitrides. Neutron diffraction is essential here, as the X-ray scattering factors of oxygen and nitrogen are not sufficiently different to permit the two atoms to be distinguished. Among the oxynitrides studied by neutron diffraction, only a few are shown to exhibit an ordered nitrogen/oxygen arrangement: this is the case, for instance, of TaON [12] with ZrO_2 baddeleyite structure, or Nd_2AlO_3N [13] and Sr_2TaO_3N [14] with K_2NiF_4-type structure.

In this work we have studied the partial nitridation of the pyrochlore $Y_2Mo_2O_7$. This material was first described by Hubert [10] and Subramanian *et al.* [16] and it has recently been the topic of a number of studies concerning its spin-glass characteristics due to geometrical frustration [17–20]. In this paper, we report on the preparation of an oxynitride of composition $Y_2Mo_2O_{4.5}N_{2.5}$ obtained by ammonolysis of $Y_2Mo_2O_7$, and its characterization by neutron powder diffraction (NPD), thermal analysis and magnetic measurements.

Experimental Section

Stoichiometric amounts of analytical grade MoO_2 and Y_2O_3 were mixed in an agate mortar. The sample was slowly heated up to 1650 K and annealed at this temperature for 12 h in a nitrogen flow. This procedure yielded the $Y_2Mo_2O_7$ pyrochlore in polycrystalline form, pure to X-ray diffraction analysis (PRF file 84-1535). For the synthesis of the oxynitride, the precursor $Y_2Mo_2O_7$ powder was placed in an alumina boat and annealed under flowing ammonia at 898 K for 22 h followed by slow cooling of the furnace to room temperature.

Thermal analysis was carried out in a Mettler TA3000 system equipped with a TC10 processor unit. Thermogravimetric (TG) curves were obtained in a TG50 unit, working at a heating rate of 10 °C min^{-1}, in an air flow of 0.3 l min^{-1}. About 60 mg of the oxynitride sample were used in the experiment.

The product was initially characterized by XRD (Cu-K_α, $\lambda = 1.5406$ Å) for phase identification and to assess phase purity. For the structural refinement, a NPD pattern was collected at room temperature at the high-resolution D2B diffractometer (ILL-Grenoble). The high-flux mode was used. About 3 g of sample were contained in a vanadium can; a collecting time of 1 h was required. A wavelength of 1.594 Å was selected from a Ge monochromator. The refinement of the NPD data was performed by the Rietveld method, using the FULLPROF refinement program [21]. A pseudo-Voigt function was chosen to generate the line shape of the diffraction peaks. The following parameters were refined in the final runs: scale factor, background coefficients, zero-point error, pseudo-Voigt corrected for asymmetry parameters, positional coordinates, mixed O and N occupancies and isotropic displacement factors for all the atoms. The coherent scattering lengths for Y, Mo, O and N were 7.75, 6.72, 5.803 and 9.36 fm, respectively.

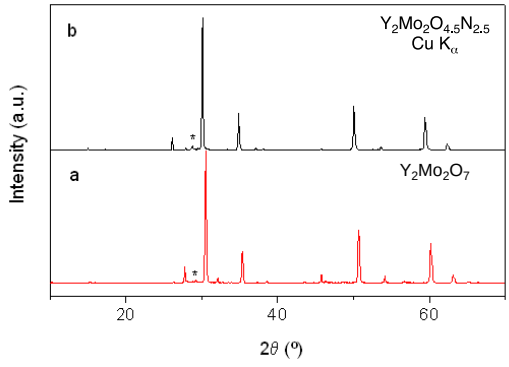

Fig. 1. XRD patterns for a) the parent $Y_2Mo_2O_7$ pyrochlore oxide, cubic with $a = 10.230(1)$ Å, and b) $Y_2Mo_2O_{4.5}N_{2.5}$ pyrochlore, cubic with $a = 10.3350(2)$ Å. The star corresponds to the most intense reflections of an Y_2MoO_5 impurity.

The magnetic susceptibility was measured with a commercial SQUID magnetometer on powdered samples, in the temperature range 5–320 K.

Results and Discussion

$Y_2Mo_2O_7$ was obtained as a black, well crystallized powder; its XRD diagram is shown in Fig. 1a. The pattern is indexed in a face-centered cubic unit cell with $a = 10.2399(5)$ Å, in agreement with literature (for instance, $a = 10.230(1)$ Å in Ref. [22]). The ammonolysis of $Y_2Mo_2O_7$ produced a dark-brown powder, with an X-ray powder diffraction pattern, shown in Fig. 1b, also characteristic of a pyrochlore phase, with clearly shifted reflections towards lower 2θ angles, corresponding to an increased unit-cell dimension of $a = 10.3350(2)$ Å. A minor impurity phase was identified as Y_2MoO_5 (PDF file 17-0593).

The nitrogen content was investigated by a subsequent analysis of the NPD data. The use of neutron

Table 1. Details of the Rietveld refinement for $Y_2Mo_2O_{4.5}N_{2.5}$ from NPD data at 295 K.

Space group	$Fd\bar{3}m$ (origin at $\bar{3}m$)
a	10.3350(2) Å
V	1103.91(4) Å^3
ρ_{calc}	5.74 g cm^{-3}
Measurement range	$10 \leq 2\theta \leq 160°$
Data points	3186
Reflections	70
Refined parameters	28
χ^2	1.72
R_p(%)	3.92
R_{wp}(%)	5.12
R_{exp}(%)	3.91
R_I(%)	3.74

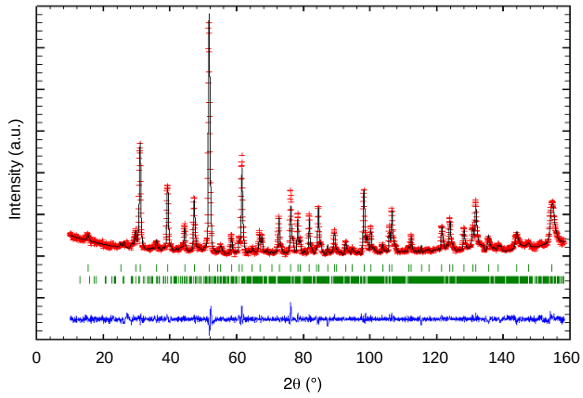

Fig. 2. Observed (crosses), calculated (full line) and difference (bottom) NPD Rietveld profiles for $Y_2Mo_2O_{4.5}N_{2.5}$ at room temperature. The two series of tick marks correspond to the allowed Bragg reflections for the main phase and the Y_2MoO_5 impurity.

Table 2. Positional and displacement parameters of $Y_2Mo_2O_{4.5(1)}N_{2.5(1)}$ at 295 K.

Atom	Site	x	y	z	B(Å^2)	f_{occ}
Y	16*c*	0	0	0	2.09(5)	1
Mo	16*d*	1/2	1/2	1/2	0.86(4)	1
O1	48*f*	0.4210(2)	1/8	1/8	4.15(7)	0.62(2)
N1	48*f*	0.4210(2)	1/8	1/8	4.15(7)	0.38(2)
O2	8*a*	0.125	1/8	1/8	0.13(7)	0.79(2)
N2	8*a*	0.125	1/8	1/8	0.13(7)	0.21(2)

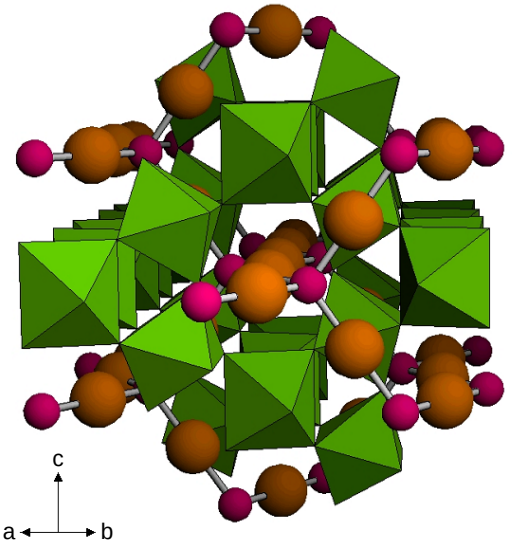

Fig. 3. Schematic representation of the crystal structure of $Y_2Mo_2O_{4.5}N_{2.5}$, approximately projected along the [110] direction, showing the linkage between six-coordinated $Mo(O1,N1)_6$ units. Large and small spheres represent Y atoms and (O2,N2) oxygen atoms, respectively.

powder diffraction to determine the site occupancy of oxygen and nitrogen is possible because of the large difference in the coherent neutron scattering lengths for both atoms, 9.36 and 5.803 fm for N and O, respectively. The crystal structure refinement was performed from the D2B high resolution data collected at room temperature and with a wavelength $\lambda = 1.594$ Å. The Rietveld refinement was carried out in the space group $Fd\bar{3}m$ (origin at $\bar{3}m$); in a previous run the crystal structure of the parent oxide $Y_2Mo_2O_7$ was modelled with yttrium atoms located at 16*c* (0,0,0) sites, molybdenum at 16*d* (1/2,1/2,1/2) positions, and the two kinds of oxygen atoms at 48*f* (x,1/8,1/8) and 8*a* (1/8,1/8,1/8). The minor impurity phase Y_2MoO_5 was included as a second phase in the refinement. A Bragg-R factor of 9.8% was obtained for this preliminary model. In a second step, nitrogen atoms were introduced at random at both oxygen positions and the mixed occupancy was refined independently at each site; the discrepancy factor significantly dropped to $R_{Bragg} = 3.92\%$. The good agreement between the observed and calculated NPD patterns after the refinement is shown in Fig. 2. No additional reflections or deviation of the space group symmetry, which could have indicated the presence of a superstructure due to long range O/N ordering, was observed. The details of the Rietveld refinement are given in Table 1. The final atomic positions and thermal parameters are reported in Table 2. A view of the crystal structure is shown in Fig. 3.

The refined composition is $Y_2Mo_2O_{4.5(1)}N_{2.5(1)}$. This formula implies a nominal oxidation state for Mo of +5.25. The larger lattice parameters for this oxynitride ($a = 10.3352(2)$ Å) compared to that of the pyrochlore $Y_2Mo_2O_7$ ($a = 10.230(1)$ Å) [22] reflects the result of the competing effects of the expan-

Table 3. Main bond distances (Å) and selected angles (°) in $Y_2Mo_2O_{4.5}N_{2.5}$, compared with those of $Y_2Mo_2O_7$ from Ref. [22].

		$Y_2Mo_2O_{4.5}N_{2.5}$	$Y_2Mo_2O_7$
Y-(O1,N1)	×6	2.542(1)	2.452
Y-(O2-N2)	×2	2.2370(1)	2.215
Mo-(O1,N1)	×6	2.001(1)	2.021
Mo-(O1,N1)-Mo		131.84(3)	126.97

sion of the volume due to the introduction of larger N^{3-} anions ($r_i = 1.46$ Å in fourfold coordination) [23] replacing the smaller O^{2-} anions ($r_i = 1.38$ Å) [23] and the decrease of the volume due to the oxidation of Mo^{4+} ($r_i = 0.65$ Å) to $Mo^{5.25+}$ (weighed average between Mo^{6+} and Mo^{5+}, $r_i = 0.605$ Å) [23]. The large isotropic displacement parameters observed for (O1,N1) atoms certainly arise from the random distribution of O and N anions over the same crystallographic positions. The 48*f* site has a variable *x* atomic parameter which is probably slightly different at the local O or N positions, giving rise to a smearing of the scattering density which is translated as a large overall displacement parameter.

Table 3 includes the mean interatomic distances and some selected bond angles, in comparison with those of $Y_2Mo_2O_7$ reported in Ref. [22]. It is noteworthy that Y-(O,N) distances increase in the oxynitride, due to the increment in the average size of the (O^{2-}, N^{3-}) anion, whereas Mo-(O,N) bond lengths are virtually unchanged, since the expansion of the anionic substructure is compensated by the oxidation and reduction in size of the Mo cations. The superexchange Mo-(O,N)-Mo angle significantly increases in the oxynitride, which has important consequences in the magnetic properties, as discussed below.

Thermal analysis of $Y_2Mo_2O_{4.5}N_{2.5}$

The thermal analysis curves are displayed in Fig. 4. The TG and DTG curves recorded under oxidizing conditions with a constant heating rate of 10 °C min^{-1} show that $Y_2Mo_2O_{4.5}N_{2.5}$ is stable in air up to 720 K; above this temperature an overall oxidation process develops, giving rise to a final weight gain, above 1000 K, of 7.5(1)%. This weight gain probably results from at least two overlapping processes, as suggested by the DTG curve that exhibits a broad shoulder centered at 893 K and a main DTG peak at 947 K. The final product at 1050 K was identified by X-ray diffraction as a mixture of Y_2O_3 and MoO_3. The transformation of

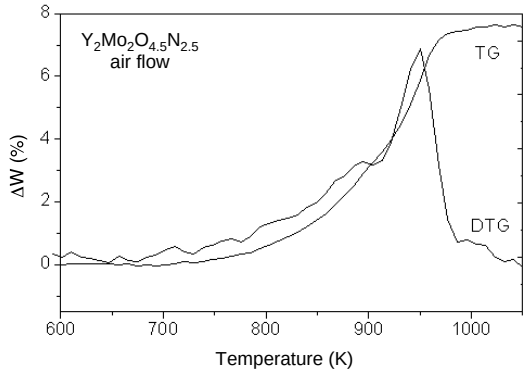

Fig. 4. Thermal analysis (TG and DTG) curves for $Y_2Mo_2O_{4.5}N_{2.5}$ in an oxidizing air flow, with a heating rate of 10 °C min^{-1}.

$Y_2Mo_2O_{4.5}N_{2.5}$ to the mentioned products, according to the chemical equation

$$Y_2Mo_2O_{4.5}N_{2.5} + 2.25\ O_2 \rightarrow Y_2O_3 + 2\ MoO_3 + 1.25\ N_2$$

implies a nominal weight gain of 7.76%, in reasonable agreement with the observed value. We do not discard that the N elimination could partially occur through chemical reaction with water vapour, producing some ammonia instead of nitrogen, although the mass balance of the thermal analysis curve would not be affected by this alternative mechanism.

Magnetic properties

The susceptibility and reciprocal susceptibility *vs* temperature data are shown in Fig. 5. In the temperature region above 150 K the zero-field cooled (ZFC) and field cooled (FC) susceptibility plots virtually coincide, exhibiting the thermal evolution expected for a paramagnetic material. At low temperatures, two anomalies in the thermal variation of the susceptibility must be highlighted: at 61 K a change of slope in both susceptibility curves could indicate the onset of a weak ferromagnetic state. A second anomaly at 24 K is observed as a maximum in the ZFC susceptibility curve, which is almost suppressed in the FC plot. Such difference between the ZFC and FC plots suggests the presence of a spin-glass-like system, as discussed below. The ZFC magnetic susceptibility data were analyzed with the equation:

$$\chi(T) = \chi_0 + C/(T - \theta)$$

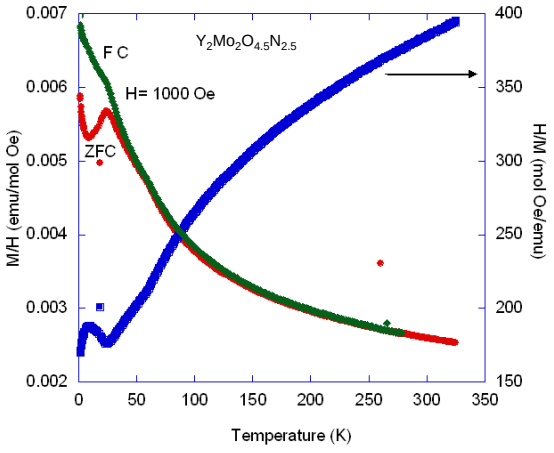

Fig. 5. Temperature variation of the magnetic susceptibility (left axis) recorded with zero-field cooled (ZFC) and field cooled (FC) conditions; the right axis corresponds to the reciprocal ZFC susceptibility.

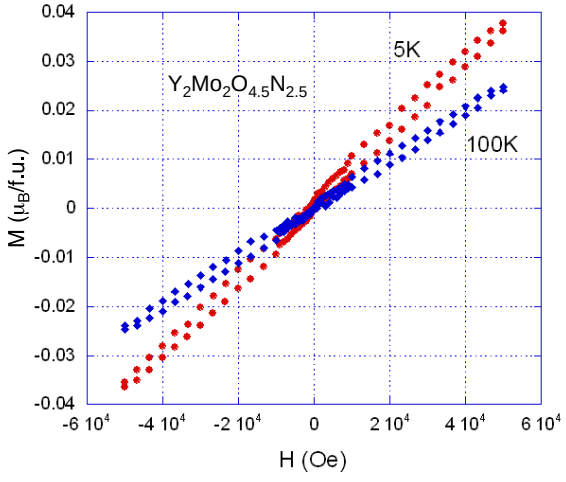

Fig. 6. Isothermal magnetization *vs.* magnetic field loops for T = 5 K and 100 K.

where χ_0 is a temperature-independent Pauli-like term. From the fit to the equation we obtain $\chi_0 = 1.85 \times 10^{-3}$ emu mol^{-1} Oe^{-1}, C = 0.21 K emu mol^{-1} Oe^{-1} and $\theta = 97$ K. The positive Weiss constant indicates that the exchange interactions are predominantly ferromagnetic in origin. From the Curie constant, an effective paramagnetic moment of 1.30 μ_B/f.u. is obtained, which corresponds to 0.92 μ_B per Mo cation. The composition of this oxynitride, refined by neutron diffraction as $Y_2Mo_2O_{4.5}N_{2.5}$, implies an average oxidation state of +5.25 for Mo cations. The corresponding 0.75 unpaired electrons would yield a Curie paramagnetic moment of 1.15 μ_B per Mo; this is in reasonable agreement with the experimental data, if we take into account that a fraction of the unpaired electrons is delocalized and gives rise to the temperature independent susceptibility term. The magnetization isotherms at 5 K (Fig. 5) show an almost linear behavior, although a small hysteresis is observed in the magnetic field cycle, consistent with the presence of a very weak ferromagnetism in the system, of 0.035 μ_B/f.u. at the maximum field of 5 T. The hysteretic behaviour is much reduced in the 100 K isotherm.

It is interesting to compare the described magnetic results for this oxynitride with those of the parent oxide, $Y_2Mo_2O_7$. From magnetic measurements and neutron diffraction data, this oxide has been described as a spin-glass system [17–20], due to the geometrically frustrated nature of the antiferromagnetic interactions, with a freezing temperature of $T_g = 22.5$ K, indicated by a clear break between FC and ZFC susceptibilities [19]. On the other hand, the compounds of the $RE_2Mo_2O_7$ (RE = rare earths) series exhibit [24] a magnetic ground state varying from a spin-glass to a ferromagnetic state as a function of the rare-earth size. It has been shown that larger RE^{3+} cations promote ferromagnetic Mo-O-Mo interactions by virtue of a broader bandwidth, which is the result of a more open Mo-O-Mo angle. The opening of this superexchange angle is driven by the concomitant increase of the unit-cell parameter, which takes a value of about 10.33 Å at the crossover between ferromagnetic and spin-glass like behaviour [24]. Very interestingly, we observe in our $Y_2Mo_2O_{4.5}N_{2.5}$ oxynitride a remarkable increase of the unit-cell parameter from 10.230(1) Å for the parent $Y_2Mo_2O_7$ pyrochlore [22] to 10.3350(2) Å, accompanied by a significant opening of the superexchange Mo-O1-Mo angle from 126.97° for the oxide [22] to 131.84(3)° for the oxynitride (see Table 3). According to the arguments given in Ref. 24, the corresponding increment of the Mo-(O,N) band width could account for the appearance in the oxynitride of FM interactions (as suggested by the positive Weiss temperature and the hysteretic magnetization isotherms) accompanied by a certain level of Pauli-like electron delocalization (χ_0 term), which is enhanced by the more strongly covalent Mo-N-Mo interaction. The unit-cell parameter of $Y_2Mo_2O_{4.5}N_{2.5}$ closely corresponds to that of the ferromagnetic-to-spin-glass crossover observed in the $R_2Mo_2O_7$ series [24]; in fact, the oxynitride exhibits a

reminiscent spin-glass character from the parent compound, which could additionally be promoted by the random distribution of O and N over the same crystallographic sites.

Conclusions

We have prepared a new oxynitride with pyrochlore structure, by ammonolysis of the parent $Y_2Mo_2O_7$ oxide. Neutron powder diffraction data allowed us to determine the N contents and its distribution over the anionic substructure: N atoms are shown to be distributed at random at both O1 and O2 crystallographic positions. The crystallographic formula, $Y_2Mo_2O_{4.5}N_{2.5}$, suggests an average oxidation state of $+5.25$ for Mo cations, assuming full electron transfer to O^{2-} and N^{3-} anions. The results of the magnetic measurements are characteristic of a spin-glass material with a weak ferromagnetism effect at low temperatures: such a behaviour is concomitant with the observed increase of the superexchange Mo-(O,N)-Mo angle and the strengthening of the Mo-N interactions with respect to the parent oxide, which delocalize the Mo-4d electrons and give rise to a temperature-independent Pauli-like susceptibility term.

Acknowledgements

We thank for the financial support of Spanish CICyT, to the project MAT 2004-0479, and we are grateful to ILL for making all facilities available.

[1] M. A. Subramanian, G. Aravamudan, G. V. Subba Rao, Prog. Solid State Chem. **15**, 55 (1983).
[2] Y. Shimakawa, Y. Kubo, T. Manako, Nature (London) **379**, 53 (1996).
[3] M. A. Subramanian, B. H. Toby, A. P. Ramirez, W. J. Marshall, A. W. Sleight, G. H. Kwei, Science **273**, 81 (1996).
[4] J. Pannetier, J. Lucas, Mater. Res. Bull. **5**, 797 (1970).
[5] D. Bernard, S. Le Montaguer, J. Pannetier, J. Lucas, Mater. Res. Bull. **6**, 75 (1971).
[6] R. Marchand, Y. Laurent, J. Guyader, P. L'Haridon, P. Verdier, J. Eur. Cer. Soc. **8**, 197 (1991).
[7] F. Pors, R. Marchand, Y. Laurent, J. Solid. State Chem. **107**, 39 (1993).
[8] V. A. Dolgikh, E. A. Lavut, Russ. J. Inorg. Chem. **36**, 1389 (1991).
[9] G. M. Veith, M. Greenblatt, M. Croft, J. B. Goodenough, Mater. Res. Bull. **36**, 1521 (2001).
[10] A. F. Wells, Structural Inorganic Chemistry, 5th edn., p. 836, Clarendon Press, Oxford (1984).
[11] M. T. Weller, S. J. Skinner, Int. J. Inorg. Mater. **2**, 463 (2000).
[12] D. Armytage, B. E. F. Fender, Acta Crystallogr. **B30**, 809 (1974).
[13] R. Marchand, R. Pastuszak, Y. Laurent, G. Roult, Rev. Chim. Mineral **19**, 684 (1982).
[14] N. Diot, R. Marchand, J. Haines, J. M. Léger, P. Macaudière, S. Hull, J. Solid State Chem. **146**, 390 (1999).
[15] P. H. Hubert, Bull. Soc. Chim. Fr. 2463 (1975).
[16] M. A. Subramanian, G. Aravamudan and G. V. Subba Rao, Mater. Res. Bull. **15**, 1401 (1980).
[17] N. Ali, M. P. Hill, S. Labroo, J. E. Greedan, J. Solid State Chem. **83**, 178 (1989).
[18] J. E. Greedan, N. P. Raju, A. Maignan, C. Simon, J. S. Pedersen, A. M. Niraimathi, E. Gmelin, M. A. Subramanian, Phys. Rev. B **54**, 7189 (1996).
[19] B. D. Gaulin, J. S. Gardner, S. R. Dunsiguer, Z. Tun, M. D. Lumsden, R. F. Kiefl, N. P. Raju, J. N. Reimers, J. E. Greedan, Phys. B: Cond. Matter **241 – 243**, 511 (1997).
[20] J. S. Gardner, G. Ehlers, R. H. Heffner, F. Mezei, J. Magn. Magn. Mater. **226 – 230**, 460 (2001).
[21] J. Rodríguez-Carvajal, Physica B **192**, 55 (1993).
[22] J. N. Reimers, J. E. Greedan, M. Sato, J. Solid State Chem. **72**, 390 (1988).
[23] R. D. Shannon, Acta Crystallogr. **A32**, 751 (1976).
[24] T. Katsufuji, H. Y. Hwang, S.-W. Cheong, Phys. Rev. Lett. **84**, 1998 (2000).